

TOPCHEM – Periodic Report: Additional Information

Fig.1

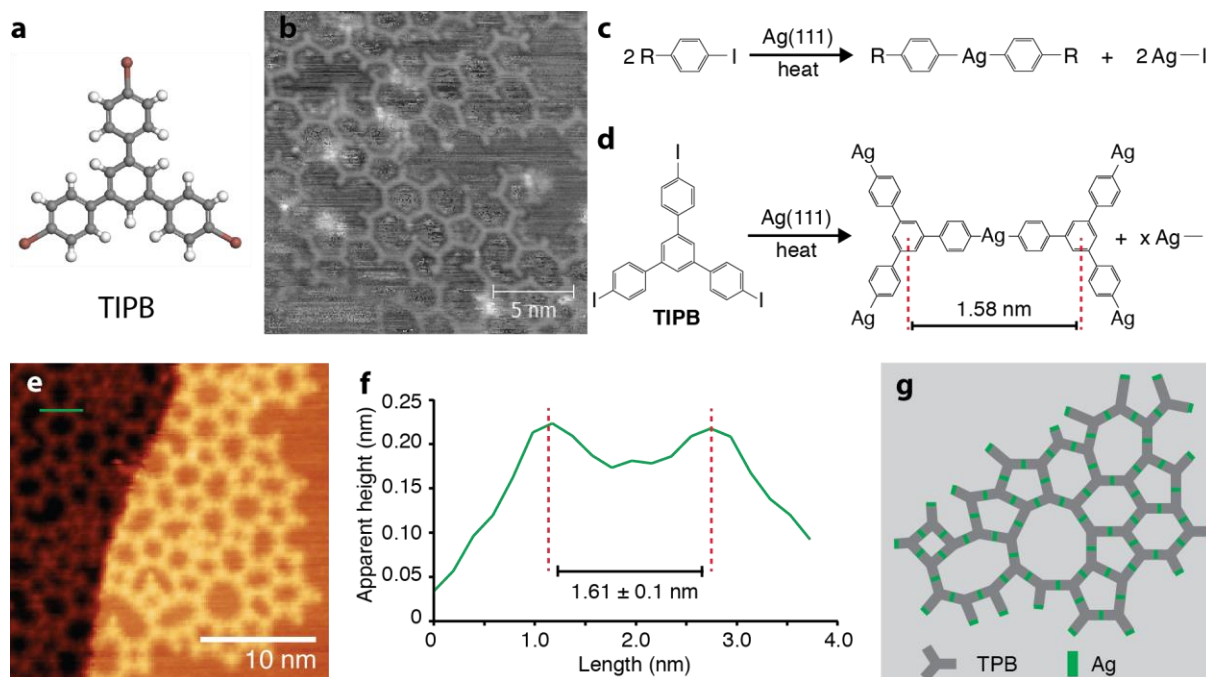


Fig. 1: On-surface reaction of TIPB (1,3,5-tris(4-iodophenyl)benzene) on Au(111) and Ag(111). (a) Chemical structure of TIPB. (b) STM image showing the structures formed after the reaction of TIPB on Au(111). (c) Scheme of Ullman-type coupling reaction where a metal-organic intermediate structure is produced. (d) Chemical structure of TIPB and the proposed scheme for formation of the 2D-MOF (e) STM image showing the extended 2D-MOF formed from TIPB on Ag(111). (f) Line-profile of the TPB-Ag-TPB bond (position of line profile indicated in (e)). (g) Schematic showing the structure of the 2D-MOF cellular network. Images in (b) and (e) acquired at room temperature under UHV conditions. Image parameters:  $V(\text{sample-bias})=+1.8\text{V}$ ,  $I(\text{set-point})=50\text{pA}$ .

Fig.2

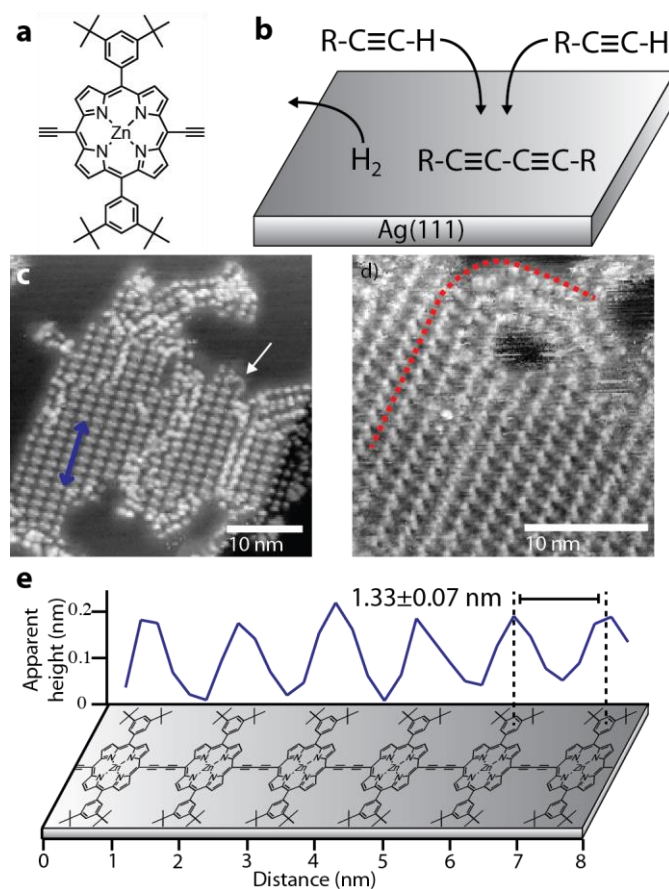


Fig. 2: On-surface Glaser coupling reaction of functionalised porphyrin monomers (1D-Porph) on Ag(111). (a) Chemical structure of porphyrin monomer (1D-Porph). (b) Scheme for on-surface reaction. (c) STM image of close-packed 1D polymer islands after deposition and annealing at 120°C (blue arrow shows row direction and position of line-profile in (e), white arrow shows 'hair-pin' bend). (d) STM image of a close-packed island; linear to curved transition indicated. (e) Line-profile acquired from (c) with dimensions and polymer model. Images in (b) and (c) acquired at room temperature under UHV conditions. Image parameters: V(sample-bias)=-1.8V, I(set-point)=30pA.

Fig.3

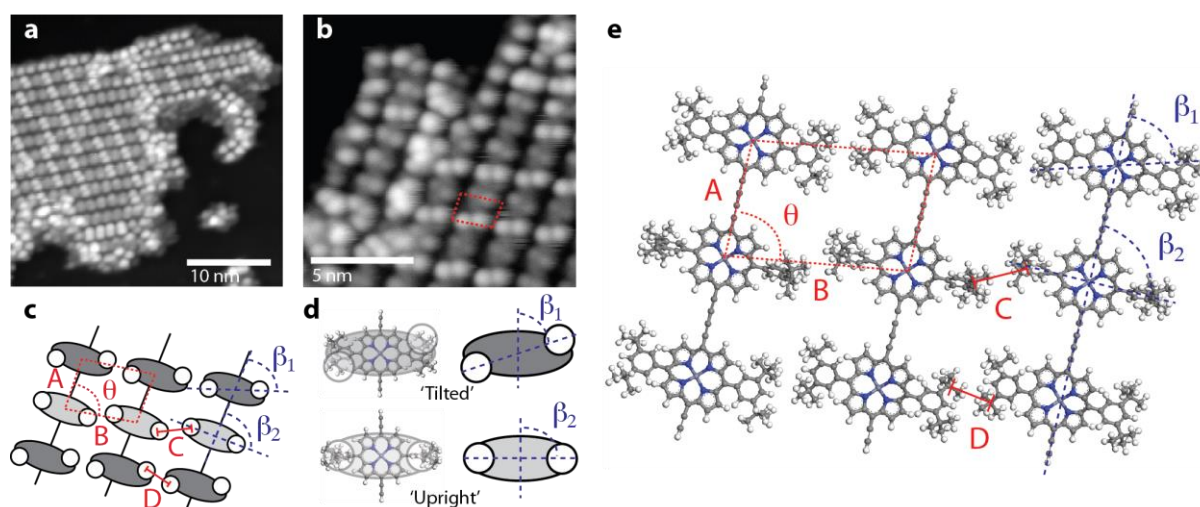


Fig. 3: Characterisation of 1D polymer chains by LT STM. STM images showing (a) structure of close-packed islands, and (b) sub-molecular resolution; porphyrin lattice indicated. (c) Scheme showing observed sub-molecular features and porphyrin lattice. (d) Molecular structure and schematics for the two conformers. (e) Molecular model of the close-packed islands formed from polymer chains. Images acquired at low-temperature ( $T = 78 \text{ K}$ ) under UHV conditions. Image parameters: (a) tunnel current,  $I = 10 \text{ pA}$ , sample voltage  $V = -1.0 \text{ V}$ , (b) tunnel current,  $I = 2 \text{ pA}$ , sample voltage,  $V = -1.5 \text{ V}$ .

Fig.4

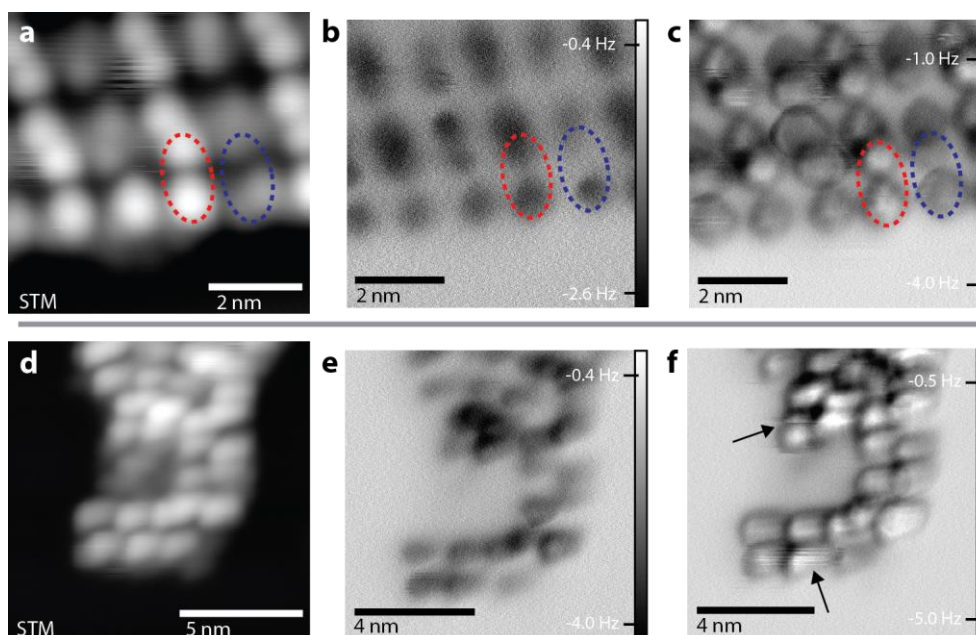


Fig. 4: Characterisation of islands and curved chains by nCAFM. (a) STM image of a close-packed island. (b and c) Same area as in (a) measured with nCAFM; tip-sample separation is decreased by 0.05 nm from (b) to (c). (d) STM image of a curved chain. (e and f) nCAFM images of a curved chain; the tip-sample separation is decreased by 0.05 nm from (e) to (f). Images acquired at low-temperature ( $T = 78$  K) under UHV conditions. Image parameters: (a and d) STM – tunnel current,  $I = 10$  pA, sample voltage,  $V = -1.8$  V, (b, c, e and f) nCAFM – constant height, sample voltage, (b and c)  $V = +0.01$  V, (e and f)  $V = 0$  V.

Fig.5

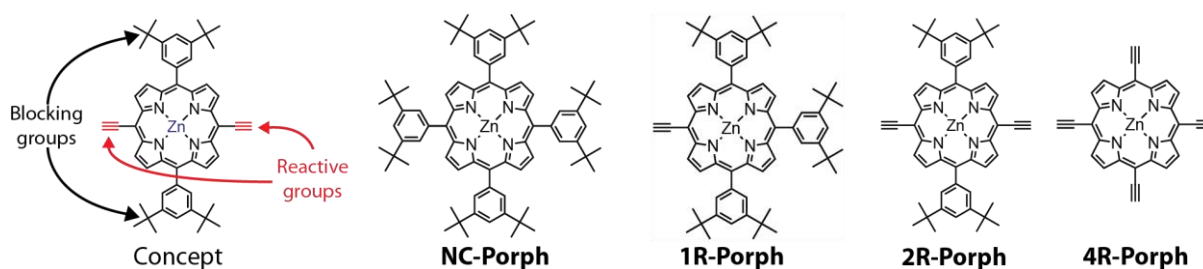


Fig. 5: Chemical structures of additional functionalised porphyrins. The tBu-based blocking groups and reactive acetylene groups are indicated. Altering the structure of the monomer units should allow covalently bonded structure with different geometries to be synthesised (e.g. the 4R-Porph variant should facilitate the growth of a 2D square lattice).

Fig.6

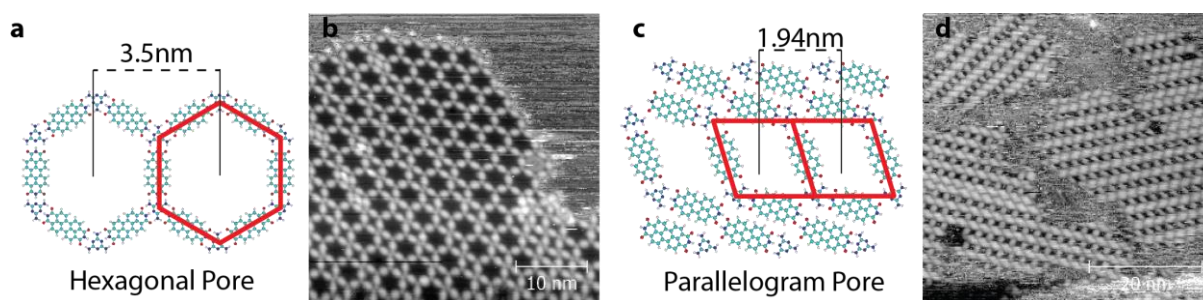


Fig. 6: Formation of hexagonal and parallelogram PTCDI-melamine hydrogen-bonded supramolecular structures on Ag(111) and Au(111). (a) Structure of PTCDI-melamine hexagonal network. (b) STM image showing the hexagonal network formed on Ag(111). (c) Structure of PTCDI-melamine parallelogram network. (d) STM image showing the parallelogram network formed on Au(111). Images in (b) and (c) acquired at room temperature under UHV conditions.

Fig.7

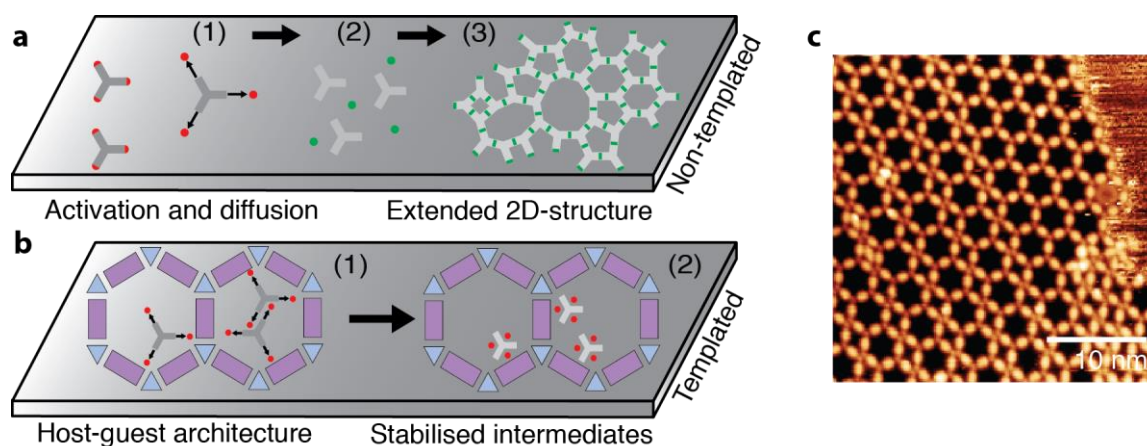


Fig. 7: Confinement of an on-surface reaction within a PTCDI-melamine porous hexagonal network on Ag(111). Scheme showing the implementation of a templated catalytic surface to control the progression of an on surface reaction. (a) In the case of the formation of the TIPB-Ag 2D-MOF there are three steps in the reaction (1) Activation of the TIPB molecule by the catalytic cleaving of the C-I bond. (2) Diffusion and (3) combination with Ag atoms to form the MOF. (b) For the templated catalytic surface the initial step, (1), continues as in the non-templated case. The formation of the extended 2D-MOF is inhibited within the pore, (2), and the reactive TPB intermediate is stabilised. (c) STM image showing the hexagonal network formed from PTCDI-melamine on Ag(111). Image acquired at room temperature under UHV conditions. Image parameters:  $V(\text{sample-bias})=+1.8\text{V}$ ,  $I(\text{set-point})=50\text{pA}$ .

Fig.8

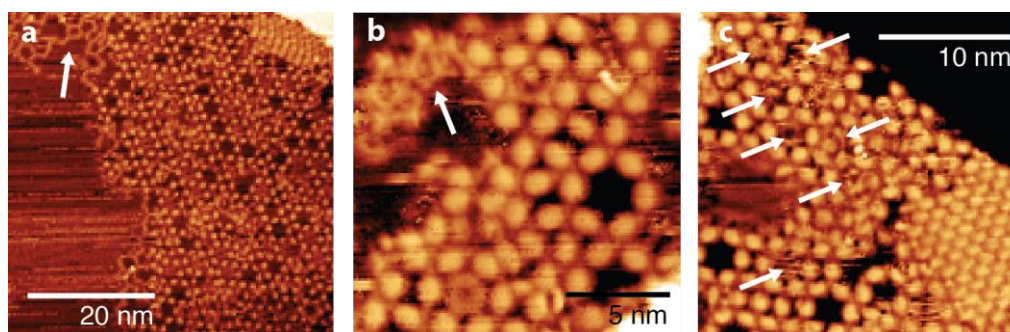


Fig. 8: Use of a templated catalytic surface to control the progression of an on-surface reaction. (a) STM image showing a domain of the PTCDI-melamine hexagonal porous network with co-deposited TIPB, a region of TPB-Ag is indicated by a white arrow. (b) STM image showing region of network structure with MOF formed from TIPB present outside of the network. (c) STM image with filled pores indicated with arrows – at RT trapped moieties diffuse continuously. Image parameters:  $V(\text{sample-bias})=-1.8\text{V}$ ,  $I(\text{set-point})=50\text{pA}$ , acquired at room temperature.

Fig.9

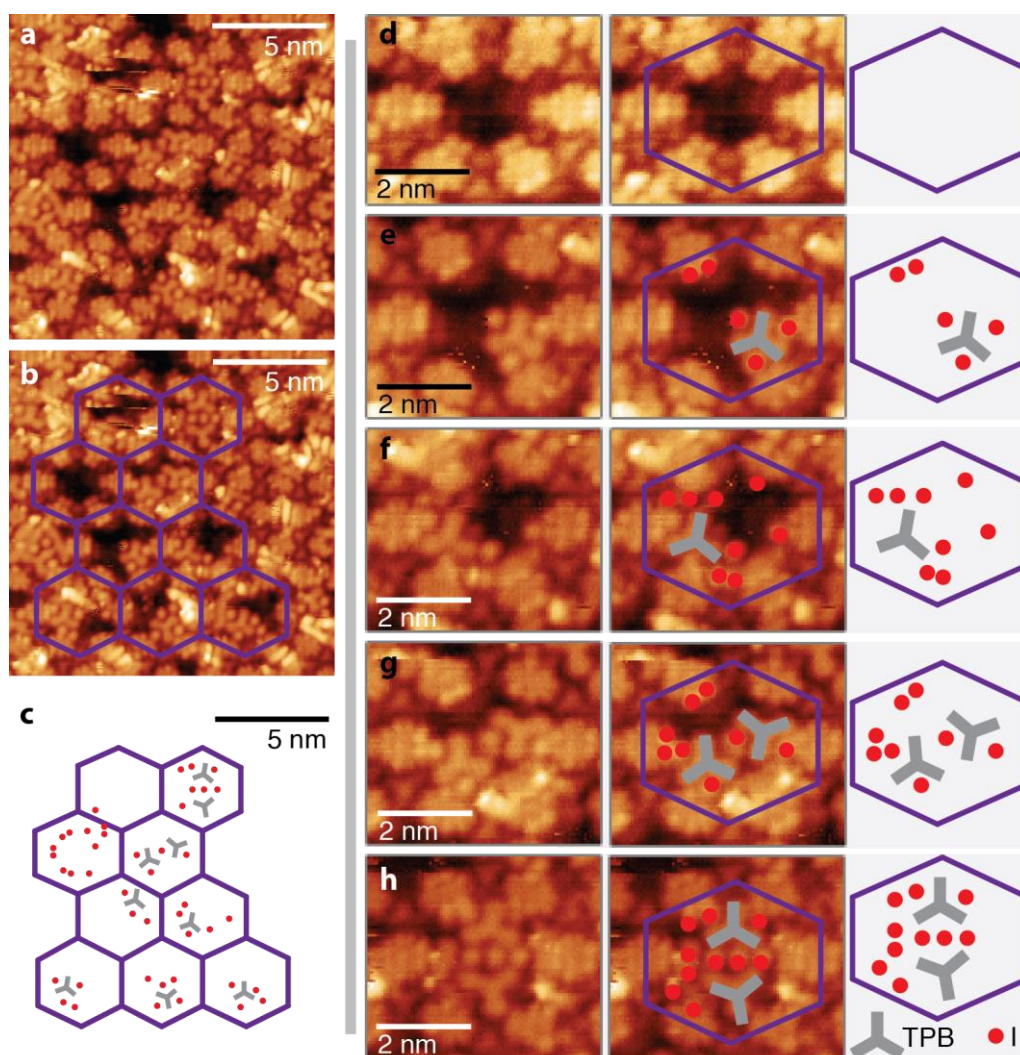


Fig. 9: Details of TIPB trapped within the pores of a PTCDI-melamine hexagonal network on Ag(111). (a) STM image (acquired at LT to limit molecular diffusion of trapped species) showing a region of PTCDI-melamine hexagonal network with trapped molecular species. (b) STM image (as in a) with the position of the hexagonal network indicated. (c) Schematic showing the position of the trapped species within the hexagonal network (as in a). (d-h) STM images of host-guest architectures within the network. The positions of dissociated TIPB (TPB) and iodine atoms are indicated. Image parameters:  $V(\text{sample-bias}) = -1.8 \text{ V}$ ,  $I(\text{set-point}) = 10 \text{ pA}$ , acquired at  $\sim 78 \text{ K}$ .

**Fig.10**

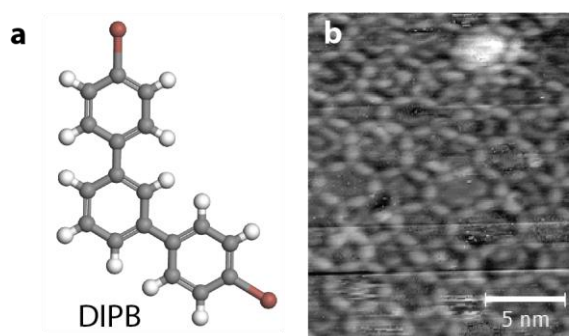


Fig. 10: PTCDI-melamine hexagonal networks on Ag(111) used to influence the on-surface reaction of DIPB. (a) Chemical structure of DIPB (1,3-di(4-iodophenyl)benzene). (b) STM image showing a region of PTCDI-melamine network on Ag(111) with DIPB species trapped within the pores. Image acquired at room temperature under UHV conditions. Image parameters:  $V(\text{sample-bias})=+1.8\text{V}$ ,  $I(\text{set-point})=30\text{pA}$ .

**Fig.11**

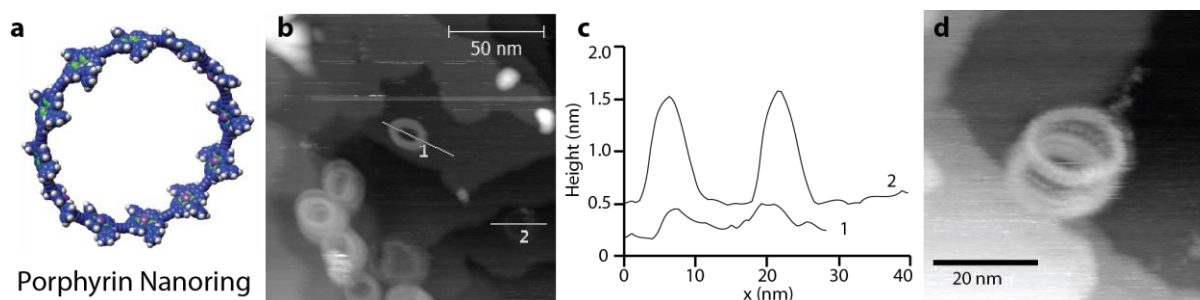


Fig. 11: Porphyrin nanorings transferred from solution to a Ag(111) surface via electrospray deposition. (a) Structure of a 12-unit porphyrin nanoring. (b) STM image showing the Ag(111) after deposition of a 30-unit porphyrin nanoring. (c) Line profiles of the nanorings (position of line-profiles shown in (b)) demonstrating that 'stacks' of rings are present on the surface. (d) STM image showing close-up of overlapping rings. Image acquired at room temperature under UHV conditions. Image parameters:  $V(\text{sample-bias})=-1.8\text{V}$ ,  $I(\text{set-point})=30\text{pA}$ .



Fig.12

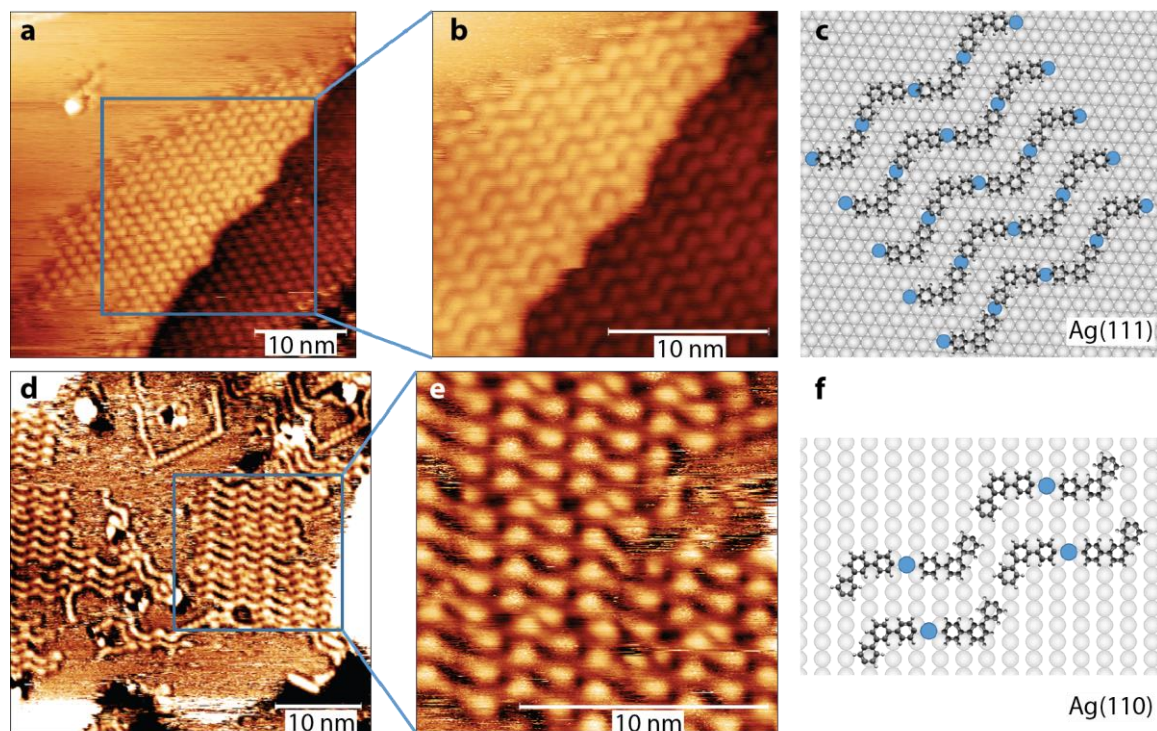


Fig. 12: Comparison of Ag(111) and Ag(110) surface with respect to the on-surface reactivity of DIPB. (a-b) STM images of DIPB on Ag(111). (c) Structure of the 1D-MOF formed from 'zig-zag' chains of reacted TIPB. (d-e) STM images of DIPB on Ag(110). (f) Structure of dimers formed from pairs of DIPB connected via single Ag adatoms on the Ag(110) surface. Image acquired at room temperature under UHV conditions. Image parameters:  $V(\text{sample-bias})=-1.5\text{V}$  to  $+1.5\text{V}$ ,  $I(\text{set-point})=5\text{pA}$ .

Fig.13

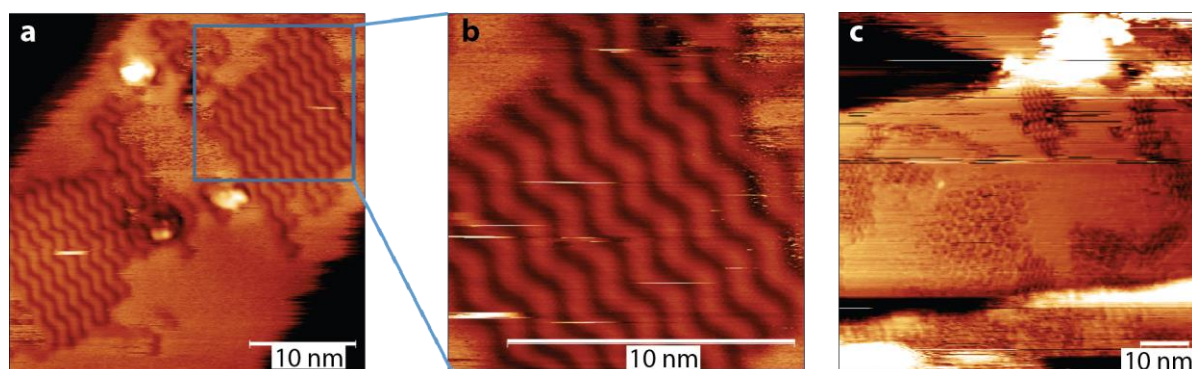


Fig. 13: Covalently bonded structures formed on Ag(111) and Ag(110) following annealing at  $120^\circ\text{C}$ . (a-b) STM images of DIPB on Ag(110) after annealing at  $120^\circ\text{C}$ : covalently bonded 'zig-zag' structures are observed. (c) STM images of DIPB on Ag(111) after annealing at  $120^\circ\text{C}$ : covalently bonded 'zig-zag' structures as well as small islands of highly-mobile hexagonal structures are observed. Image acquired at room temperature under UHV conditions. Image parameters:  $V(\text{sample-bias})=-1.5\text{V}$  to  $+1.5\text{V}$ ,  $I(\text{set-point})=5\text{pA}$ .

**Fig.14**

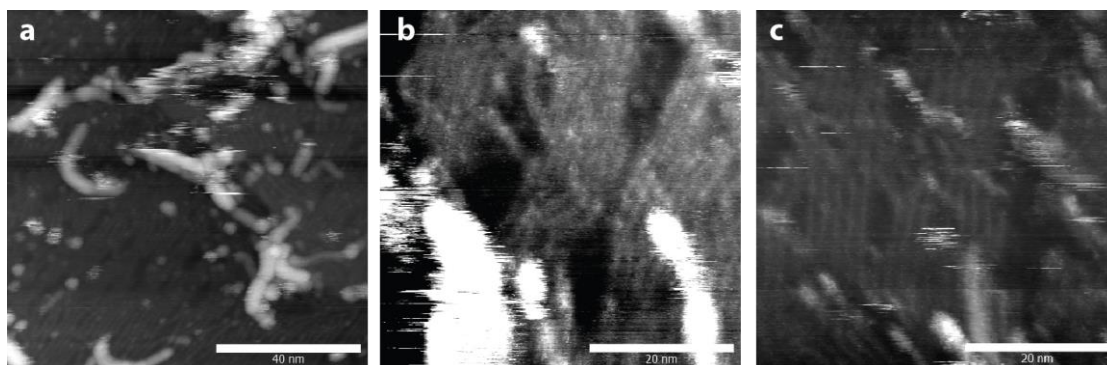


Fig. 14: Liquid-deposition of 30-unit cyclic porphyrin structure (CP-30) onto a Au(111) surface. (a-c) STM images acquired in ambient conditions of CP-30 on Au(111): Linear chain structures can be observed. Image parameters:  $V(\text{sample-bias})=+1.0\text{V}$  to  $+0.8\text{V}$ ,  $I(\text{set-point})=30\text{pA}$ .

**Fig.15**

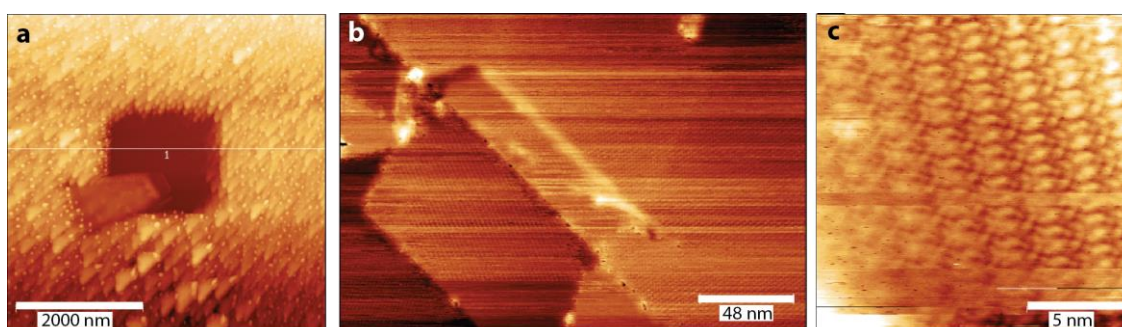


Fig. 15: AFM images of TIPB deposited onto hBN flakes supported on  $\text{SiO}_x$ . (a) AFM image showing the hBN/ $\text{SiO}_x$  surface after deposition of multilayers of TIPB; square area is tip-induced 'cleaning' of TIPB from surface, with the feature in the bottom left of the square characterised as a hBN flake. (b) AFM image of a hBN flake with periodic structure of a molecular island visible. (c) AFM image showing the molecular structure of the close-packed island.